Astron. Astrophys. 256, 148–158 (1992)

ASTRONOMY AND ASTROPHYSICS

WR 134 line-profile variability revisited ⋆

J.-M. Vreux [1], E. Gosset [1], B. Bohannan [2], and P. Conti [3]

[1] Institut d'Astrophysique, 5, avenue de Cointe, B-4000 Liège, Belgium
[2] Kitt Peak National Observatory, N.O.A.O., Tucson, AZ 85726, USA
[3] Joint Institute for Laboratory Astrophysics, University of Colorado, Boulder, CO 80309-0440, USA

Received March 13, accepted November 5, 1991

Abstract. Line profile variations of WR 134 are analyzed on more than two hundred spectra collected at Haute Provence Observatory and at Kitt Peak National Observatory. No conclusive evidence is found for a periodic behaviour. However for some frequencies [for example the ones close to $\nu = (n \times 0.5)\,\mathrm{day}^{-1}$] the data are ill-distributed, and the existence of a related periodic phenomenon cannot be completely ruled out. This does not mean that the variability presents a purely random behaviour. Several new characteristics of the observed deformations are extracted from the analysis of the spectra and it is tentatively suggested that these could be the signature of a bipolar flow.

Key words: Wolf-Rayet – spectroscopy – variable

1. Introduction

WR 134 = HD 191765 is a bright WN 6 star which is associated with a filamentary anonymous nebula embedded in the H II region S 109 (van der Hucht et al. 1981). Its radial velocity due to galactic rotation has been estimated to be of the order of $0\,\mathrm{km\,s^{-1}}$ (between -26 and $+10\,\mathrm{km\,s^{-1}}$) by Underhill et al. (1990).

According to Treffers & Chu (1982), the morphology of the associated nebula is reminiscent of the interaction of a strong stellar wind with the ambient interstellar medium [wind blown bubble in Chu et al.'s (1983) classification]. As ring nebulae around WR stars have also been suggested to be a possible indicator of a binary system with a collapsed companion (van den Heuvel 1976), WR 134 has been investigated to search for the signature of such a configuration and indeed claimed to be a Wolf-Rayet with a low-mass companion by Antokhin et al. (1982). From the analysis of their photometric data the latter announced a period of 7.44 d, which they used later to plot their radial velocity data and derive a value of the semi-amplitude K. A few years later, in the context of our reinvestigation of the so-called WR + compact systems (Vreux 1985), we made our own photometric observations of WR 134 (Vreux & Manfroid 1985) which did not support the period or the light curve presented by Antokhin et al. (1982). One year later, Moffat & Shara (1986) announced a 1.8 d period deduced from broad band photometric observations. Finally, Antokhin & Volkov (1987) present new observations performed in 1984, 1985 and 1986 (the ones performed in 1985 being compatible with ours) and conclude that the light curves of WR 134 are "variable in shape, amplitude and average light level on a long timescale". In that paper they no longer claim to have found any periodicity in the variations even if they keep mentioning a binary system.

As far as spectroscopic data are concerned, the detailed analysis of such material is the main objective of the present paper. The radial velocity plots of Antokhin et al. (1982) (with their claimed photometric period) are very noisy: typically the whole range of variation is spanned over a phase band $\Delta\phi = 0.3$ located near $\phi = 0$ (while the eccentricity is close to zero). We are unable to comment on the 1.8 d spectroscopic period found by Lamontagne (1983), since we have never had access to that reference. It should be mentioned that we perfectly agree with a later statement by Moffat et al. (1988) who consider that the change of "the line shift is not a global phenomenon but rather artificially due to fine structure changes in this line", an interpretation that we had, in fact, already suggested in the case of WR 136 (Vreux et al. 1985).

Another possible way to detect Wolf-Rayet binary systems is through polarization observations. WR 134 has been studied with such a technique by Robert et al. (1989) who conclude that "based on the polarization alone, the WR + c duplicity of HD 191765 is unlikely". Among the possible explanations for the observed polarization variability, they favour the asymmetric ejection of blobs of wind material. This is on the basis of high quality spectroscopic observations by Moffat et al. (1988), observations we will discuss in more detail later on. Robert et al. (1989) also address the important question as to whether the observed asymmetries occur in a disk or in a spherical envelope, and they mention that, among the Cygnus WR stars, WR 134 is "the object for which such a plane is most evident" but that the result depends on "only a few isolated data points". It is interesting to note that such a disk shape envelope for WR 134 had already been suggested by Schmidt (1988), in order to interpret his polarization measurements. This indication from two independent polarimetry studies has to be kept in mind when we suggest an interpretation of our data.

We will now focus on more recent studies performed with modern instrumentation allowing a precise determination of line profile variations using spectroscopic data. Indeed WR 134 exhibits spectacular line profile variations as illustrated as early as 1970 in a figure of Smith & Kuhi's paper (1970). The first

Send offprint requests to: J.-M. Vreux

⋆ All the observations discussed here were obtained at the Haute Provence Observatory and at the Kitt Peak National Observatory.

published modern attempt (i.e. time resolved, high resolution, high signal-to-noise spectroscopy) is due to Moffat et al. (1988) who interpret the profile variations they observe in WR 134 and WR 136 as due to blobs of wind material randomly ejected by the star and accelerated outwards, i.e. an interpretation similar to the one given to explain moving bumps observed in the UV resonance lines of some stellar spectra (Lamers et al. 1988).

This interpretation has been questioned in the second modern study by Underhill et al. (1990). They claim that their data "do not show systematic changes of the type which are implied by the scenario of Moffat et al.", a statement that our spectra lead us to endorse in the sense that all our observations cannot be explained in the frame of blobs accelerating outwards (see Sects. 3 and 4). Underhill and collaborators also draw attention to the "restricted velocity range, both positive and negative, within which the changing subpeaks are seen in the case of HD 191765" a remark which will be refined with our observations and then shown to have important implications. Underhill et al. (1990) interpret their observations via a rotating wheel-like structure, the "spokes" of the wheel being "filamentary, ever changing tubes of plasma which radiate chiefly lines of He II and other ions" while the rim/disk radiates He I λ5876 and He II λ5411.

The main argument Underhill et al. (1990) developed to propose a disk-like structure is the claimed double peak aspect of He I λ5876. As a matter of fact the redward peak region is perturbed by interstellar and terrestrial absorption lines, and the discussion is mainly based on the appearance of a stable blueward peak which rises to about 6% above the central mean height of He I λ5876. The difficulty we find in accepting this interpretation is that while we do observe the same profile as Underhill et al. (1990) for He I λ5876 ($2p^3P^0$–$3d^3D$), we do not observe the same aspect on other He I lines for which we have data i.e. He I λ4471 ($2p^3P^0$–$4d^3D$) and He I λ10830 ($2s^3S$–$2p^3P^0$) (the stability of the profile of He I λ10830 presented in Vreux et al., 1990 is confirmed by Eenens 1990). These lines do not exhibit a shortward emission peak but rather a classical P Cygni absorption. Consequently, we suspect that the blueward bump of He I λ5876 emission is the result of blending which also pushes up the absorption component, raising its deepest point to a level close to the one of the continuum (see Fig. 4 of Underhill et al. 1990). We will present later (Sects. 3 and 4) an argument based on the variability analysis which indicates that indeed He I λ5876 has a blueward variable absorption component. This is the reason why we do not feel irrevocably linked to a model including a rotating wheel located at some distance from the star.

After a description of the observational material (Sect. 2) the various techniques which have been applied to study the variability exhibited by the data will be reviewed (Sect. 3). It will be shown that even if the various period searches lead to no result (Sect. 3.1), important information can nevertheless be extracted from the observed variability (Sect. 3.2). Then in Sect. 4, the implications of the constraints derived in Sect. 3.2 as well as information gathered in the literature will be used to tentatively suggest a model for WR 134.

2. Observations

As soon as spectrophotographic observations of WR 134 at Haute Provence Observatory (HPO) in 1984 confirmed that the spectacular profile variations described by Smith & Kuhi (1970) were not a sporadic phenomenon, a decision was made to concentrate efforts on this object. In the light of the difficulties encountered in the analysis of the WR 136 variations (Vreux et al. 1985), it was obvious that only a large number of high quality observations could possibly lead to a trustworthy result. Also, the one-day aliasing problem would need to be addressed. Consequently a first coordinated campaign between HPO and Kitt Peak National Observatory (KPNO) was organized by JMV and BB and took place during the fall 1985. Unfortunately due to adverse meteorological conditions as well as instrumentation problems at HPO, it failed. Another effort was attempted independently at the two observatories in 1987, this time with success on both sides of the Atlantic, with the acquisition of more than two hundred CCD spectra of good quality, the two observing runs being less than two months apart. These are the data which will be discussed here.

2.1. *Haute Provence Observatory data*

The bulk of the spectra were obtained between July 29 and August 6, 1987, with continuously acceptable meteorological conditions during the eight nights of a JMV observing run. These data were complemented by a few others kindly obtained between August 7 and 10 by Mrs. Y. Andrillat during an observing run devoted to another program. All the HPO data have been obtained at the 1.93 m telescope equipped with the Carelec spectrograph in a configuration giving a spectral coverage from λ3940 to λ4430 with a reciprocal dispersion of 33 Å mm^{-1}. The detector was a RCA 512 × 323 CCD with a readout noise of about 117 e$^-$ and pixel sizes of 30 × 30 μm. For the observations we used a 365 μm slit width which corresponded to 2″.5 on the sky and 2.1 pxl on the detector. The slit length was 50 mm. More details on the instrumentation as well as on the observing procedures can be found in the HPO "notice d'utilisation du Carelec". Comparison exposures of He-Ar lamps were made each time the telescope was pointed at a new object or, at maximum, after three spectra, when the telescope was kept locked on the same target for a relatively long time. The data reduction (bias removal, flat fielding, wavelength calibration, reduction to continuum) has been performed with the ESO software system IHAP implemented at HPO and in Liège.

As usual when dealing with WR spectra, the reduction to the continuum was not straightforward due to the crowding of broad emission lines in the limited spectral range available. Of course the main concern here is not an absolute determination of the continuum but the study of line profile variations, which means that the consistency of the individual continuum fittings is most important. This has been achieved in a two step procedure. As we had no reason to expect the shape of the flat field continuum to be particularly close to the one of a WR star we have chosen to make a small detour, using an O star continuum as a first approximation. As classical standards did not offer sufficiently large continuum windows in the wavelength domain under consideration, we finally selected as reference an O star with particularly narrow (emission) lines, HD 108. Then, the "response curve" used to reduce the HD 108 spectra to continuum has been systematically applied to the WR 134 spectra. If the WR and the O star continua had the same shape, such a procedure applied to spectrophotometric data would ensure an automatic reduction to the continuum of the WR spectra (ignoring a multiplicative constant). Using this procedure we now have to obtain the ratio between a WR star continuum and an O star continuum, two functions we can expect to be relatively similar. We made the hypothesis that they were similar enough to allow us to approximate their ratio by a straight line (of unknown slope) in the wavelength domain under consideration. As a matter of fact we had no other choice than the use of a first degree polynomial as we

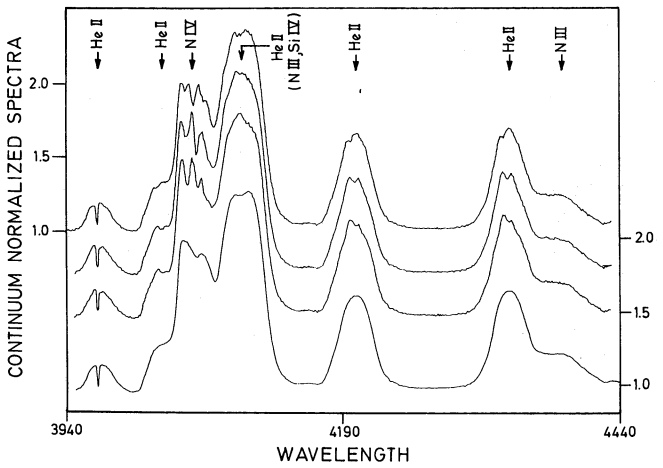

Fig. 1. The bottom spectrum is the mean of the 74 HPO spectra. The three upper ones are individual spectra obtained during the night of August 2, 1987, respectively at U.T. 20 h 26 min, 22 h 16 min and 25 h 48 min (starting from bottom). Wavelength is given in Ångström unit, as for all the following figures

hardly have two "points" to define it. On the red side, the selected region that we consider as safe is located between He II λ4200 and He II λ4339. On the blue side, as we are reluctant to use the very end of the CCD spectra, we have selected a region located between He II λ3968 and He II λ4026 even if a pollution of this region by the wings of the neighbouring He II lines is not excluded. The choice of such a procedure can be considered as justified a posteriori by the "cleanliness" of the results of the statistical analysis of the variability.

A total of 74 spectra have been obtained. A typical exposure time was of the order of 8 min (increased above 10 min only during two relatively poor nights i.e. July 29 and August 7). This was sufficient to get a S/N ranging from 330 to 400 for the continuum. With very few exceptions due to meteorological conditions, the information collected during a typical night consists of several groups (between 2 and 6) of two or three spectra distributed over the 7 h of an observing night. The spectra of each group were taken consecutively, i.e. typically at 10 min intervals. They allowed us to check that no noticeable variations occurred on such a short time scale. A typical time interval between two groups was of the order of 2 h (between 1 and 4, depending on the number of groups we decided to get during the night) as we knew that noticeable variations could occur on such a timescale.

In Fig. 1 are displayed three individual spectra as well as the mean of the 74 HPO spectra. We would like to draw attention to the profiles of the He II λ4200 and He II λ4339 lines, which are rather blend-free (except the red wing of He II λ4339). On the individual spectra a clear variable subpeak structure is visible on top of both lines. These subpeak structures are always remarkably similar for the two lines indicating that they are not due to a local blend or to an artifact of the observing technique but that they are the signature of a physical mechanism acting on the formation process of the two lines.

It is also interesting to notice the smooth and rather symmetrical aspect of the tops of the profiles of these two lines on the mean spectrum which tends to indicate that our sampling has evenly covered the ever changing aspect of the varying subpeaks' structure. The profile of the other lines is more complex, mainly due to blends, and will be discussed later on.

2.2. The Kitt Peak National Observatory data

The KPNO spectra were obtained by BB during a 12 night observing run (Sep. 23 to Oct. 4, 1987) with the Pennsylvania State fiber optic échelle (FOE) spectrograph linked to the 0.9 m coudé feed telescope. The 200 µm optical fiber of this spectrometer subtends 5″ in the image plane of the feed telescope and corresponds to 2.2 pxl on an RCA CCD with 30 µm pixels. The spectra consist of 23 orders, each about 100 Å wide, spanning a wavelength range from λ3940 Å to λ6600 Å with a spectral resolution of the order of 10000. This wavelength domain is however not fully covered since a complete spectral overlap ends near 4400 Å, after which the gaps become progressively wider toward the red. More details on this spectrometer can be found in Ramsey & Huenemoerder (1986).

Five wavelength calibrations were typically taken during the course of the night in order to check the stability of the instrumentation: no shift was detected in the dispersion direction. The data reduction has been performed with the IRAF version 2.5 package and is fully documented in the thesis of McCandliss (1988), including comments on the intricacies of échelle data handling.

The KPNO collection consists of 152 spectra for which the majority of the integration times lie between 20 and 30 min; a few integrations are as short as 15 min and only 7 spectra out of 152 have integration times longer than 30 min. During the course of a night the telescope was kept constantly pointed at WR 134 and consequently the typical time interval between two spectra was of the order of 30 min.

The coherence of HPO and KPNO wavelength scales is excellent. After taking into account the small heliocentric corrections, the wavelength of the Ca II interstellar line λ3968.5 Å was measured on the two mean spectra (i.e. HPO mean and KPNO mean) through a gaussian fitting procedure. The two results differ by about 0.1 Å, i.e. close to a tenth of an HPO pixel.

The average S/N of the KPNO data (about 125, McCandliss 1988) is nearly three times lower than the one of the HPO data. An additional source of uncertainty is linked to the observation technique itself i.e. to the use of an échelle spectrograph. It is indeed important to realize that seven orders are necessary to cover the spectral range of the HPO data. This means that six inter-orders lie well inside the wavelength domain under consideration, some of them inevitably located on emission line profiles. As careful as the data reduction has been (McCandliss 1988), at the level of accuracy we are dealing with (1%), such a situation introduces some additional uncertainties on the final global spectra. However, outside pathological regions, the KPNO mean spectrum is very similar to the HPO one, indicating that a fair sampling of the different aspects of the variable structure has been achieved in both sets of data.

3. Data analysis

3.1. In search of a period

The first search for periodicity in the variations observed in the sample under discussion was conducted on the KPNO data (McCandliss 1988). An analysis of the temporal distribution of the observations indicates that meaningful period searches can be conducted in the 1 d^{-1} to 1 h^{-1} frequency regime, the only notable exceptions being the periods around 1, 0.667, 0.5 and 0.333 d. The

same analysis shows that the possibility of finding periods between 1 d and 11 d is much more limited.

Two basic measurements were performed on the line profiles. The first one is the line center defined through the first moment of the profile, as suggested by Balona (1986). The second one, called difference flux fraction, is a relative measure of the flux variation defined by the expresssion

$$\frac{EW_i - EW_M}{EW_M}$$

where EW_i is the equivalent width of the line measured on the ith individual spectrum and EW_M the equivalent width of the same line measured on the mean spectrum M (mean of the various i). Line centers and difference flux fractions were measured for N IV λ4058, He II + N III + Si IV λ4100, He II λ4200, 4339, 4542, 4859, 5411 and 6560. Searches for periods in all the line positions and flux time series were then performed with the normalized periodogram method of Scargle (1982). The result is that no conclusive evidence can be found for a periodic behaviour on the time scales over which the distribution of data allows a meaningful period search. The line profiles are variable and, in general, the line positions are well correlated while the flux changes are not, but there is no reason to believe that any periodic phenomenon is present (McCandliss 1988).

The HPO data have been searched for periodicities in a similar manner. After a visual inspection of the various profiles had shown that no significant variation took place on a very short time scale, the spectra of a given temporal group (i.e. spectra taken less than 15 min apart, see Sect. 2) have been coadded; this leads to a series of 34 spectra. Then various measurement techniques were applied to try to quantify the observed variations.

For the line profiles themselves, these techniques have included line positions and equivalent width measurements. Line positions of the global profiles were obtained through IHAP built-in techniques (Gaussian fitting, median) as well as through cross-correlations with respect to a reference mean profile. The positions of the subpeaks visible on top of the line profiles were also measured as carefully as possible. Furthermore, to better evaluate the relative amplitudes and positions of the variations, all the spectra have been divided by the mean spectrum leading to a series of mean-normalized spectra on which we see at each wavelength (1 pxl bandwidth) the percentage of variation relative to the mean. An example of such a spectrum is given in Fig. 2 which allows one to appreciate the high S/N ratio of the data: variations of the order of one percent are clearly detected. The 1% level is also an order of magnitude we have to keep in mind: the variations under study are not dramatic ones as far as the global amount of energy emitted by the star is concerned. A montage of the HPO mean-normalized spectra (after the partial temporal binning mentioned above was applied) is displayed in Fig. 3. Again various measurements were performed on these mean-normalized spectra (positions of maxima and minima as well as first and second order moments). All these methods allow one to transform into numbers the clear variations observed on the profiles, but a period search through these numbers has been inconclusive.

As a last attempt to find a period, a brute force technique has been applied to the HPO data i.e. a temporal Fourier transform of each pixel in the series of spectra. Unfortunately (in terms of period searching) no period clearly shows up. We have a forest of peaks, nearly all of them located close to $\nu = (n \times 0.5)\,d^{-1}$ i.e. close to poorly studied frequencies due to the temporal distribution of the data. The profiles are indeed variable (which we already know) but no period can be extracted from the data.

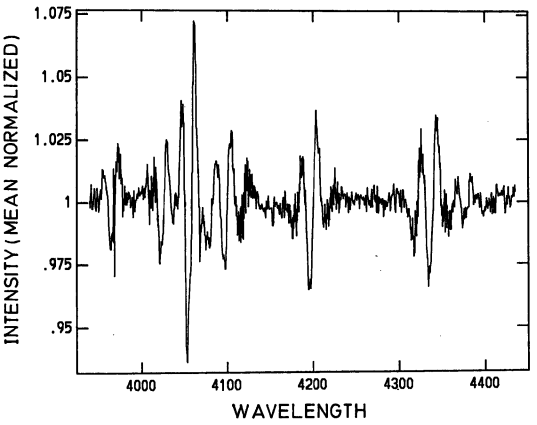

Fig. 2. Example of a mean-normalized HPO spectrum i.e. of the result of the division of an individual spectrum (here the one obtained July 31, 1987 at U.T. 23 h 46 min) by the mean spectrum. At a given wavelength, the ordinate allows to determine the percentage of deformation of the individual spectrum relative to the mean spectrum

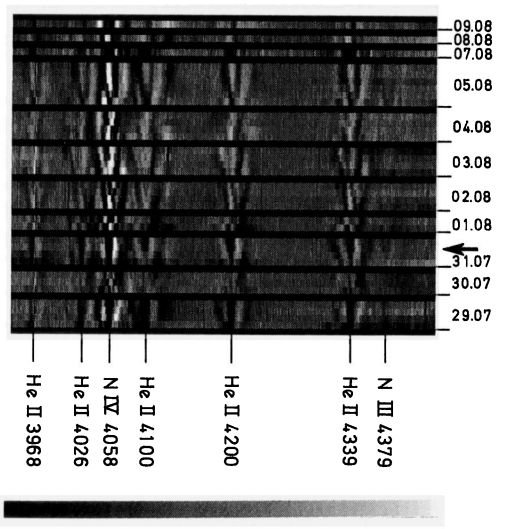

Fig. 3. Montage of the 34 (time binned) mean-normalized HPO spectra (see text). Grey corresponds to a value close to one. The various degrees of "dark" and "white" correspond to deviations from the mean spectrum (white is above average; see text and also Fig. 2). Time runs from bottom to top. The position of the spectrum of Fig. 2 is indicated by an arrow. The grey scale is given below the identification, ranging from 0.97 (darkest) to 1.05 (whitest)

A similar procedure has been applied to the KPNO data but for them the situation is much noisier for various reasons. The first ones are the intrinsically lower S/N ratios of the data and the less secure procedure to reduce the spectra to the continuum. Another (localized) source of noise is due to the inter-orders (a detailed discussion can be found in McCandliss 1988). To improve slightly that situation, and also to make the amount of data more manageable (while keeping a time resolution of the order of one hour) we made a "temporal binning" of the data. This means that the spectra have been added two by two with a few exceptions corresponding to situations where the time interval between two consecutive spectra was abnormally long for various reasons (calibrations, clouds). The application of the "brute force technique" mentioned above to the KPNO data again leads to no conclusive period.

The conclusion of this section is that the rather extensive sets of data investigated here do not allow to find the signature of a periodic phenomenon. Let us nevertheless recall that some frequencies are poorly studied and consequently that some periodicity in the variability cannot be completely ruled out.

3.2. *Characteristics of the variability*

The fact that no clear periodicity could be found in the line profile variations does not mean that the observed deformations of the mean profiles have a purely random behaviour.

For example an eye inspection of Fig. 3 – mainly its right part, which concerns a less crowded region – could give the impression of nicely repeating patterns. A closer look, however, indicates that the situation is more complex. On this figure the white color indicates an excess of intensity relative to the mean profile i.e. the white regions of a given spectrum correspond to the positive bumps in Moffat et al. (1988). In several cases, the lines linking the whitest region of successive spectra of a given night define a kind of *V* shape which is the signature of situations similar to the ones described by Moffat et al. (1988); i.e. "those bumps that start red-shifted relative to the observed line-center become even more red-shifted with time while those that start blue-shifted become more blue-shifted with time". The night of July 31 shows a rather good example of such an event. But some observations do not obey such a law. For example, during the night of August 4, the line linking the centers of the white spots located on the blue side of the line center of He II λ4339 has a slope in the "wrong" direction: a disturbance which starts blue-shifted relative to the observed line center is apparently becoming less blue-shifted with time. Using such a subjective approach, other examples of "misbehaving" disturbances can be found. Such a situation of a bump apparently no longer moving in the expected direction can also be seen in Fig. 6 of Underhill et al. (1990): the left bump of spectrum *E* has moved back relative to the position it should occupy by extrapolation of its location on the preceding spectra.

All this indicates a situation more complex than that of mere blobs gently accelerating outward, even if many events fit such a scenario. Due to that complexity the analysis of the data has to be pushed further to avoid the subjectivity of a simple eye inspection leading to descriptions such as the one above.

A look at our extensive collection of data immediately gives the impression that the variability occurs preferentially at certain fixed locations on the profile. This can be quantified through the computation and plot of a "variation spectrum" i.e. plot of the standard deviation of each individual wavelength bin of the mean-normalized spectra. The result for the HPO data is given in Fig. 4. This tracing confirms a result of McCandliss (1988) in the sense that with the HPO data we also observe a marked decrease of the variability close to the center of the lines and a higher variability of N IV λ4058 relative to the He II lines at λ4200 and λ4339 [the values plotted by McCandliss (1988) on his variation spectrum are not identical to the one plotted here due to the specificities of échelle spectra and to a different definition, but this is not important for the present discussion]. Let us stress that this central minimum is not due to the fact that we use the mean-normalized spectra: the central minimum and the two maxima which define it are well within the rather flat top of the mean profiles.

Beyond this confirmation, the higher S/N HPO data allow us to get more information in the sense that they show that the variation spectrum of a line profile does not consist of a simple double peaked profile but of a more complex structure. On the profile with the "cleanest" variations, the one of N IV λ4058, additional peaks are visible and the positions of most of them are nicely correlated with bumps in the variation spectrum of the He II λ4200 and λ4339 lines.

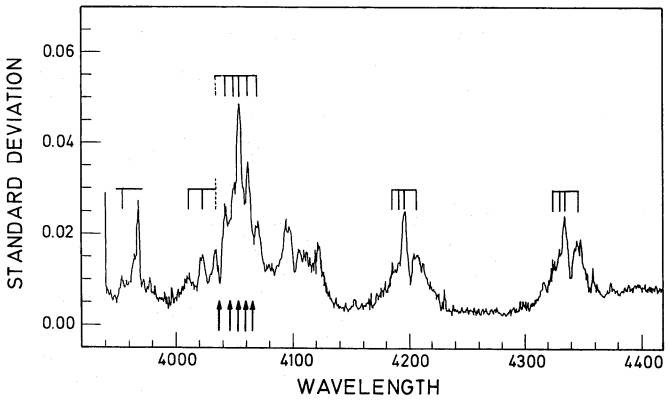

Fig. 4. Variation spectrum of HPO data i.e. distribution of the observed standard deviation around the mean-normalized spectrum as a function of wavelength (see text and Table 1). The upper marking indicates the positions of the local maxima; the lower arrows under the variation spectrum of the N IV λ4058 profile indicate the position of the local minima

Table 1. Radial velocities (in km s^{-1}) of the subpeaks observed on the variation spectrum

Mean	N IV λ4058	He II λ4339	He II λ4200	He II λ4026	He II λ3968
	(−1795)				
−1070	−1170	−980	−1020	−1125	−1060
− 625	− 615	−635	− 630		
− 290	− 280	−325	− 270	− 270	− 300
	+ 275				
		+470	+ 480	(+ 590)	
	+ 865				

On the blue side of the variation spectrum of the N IV λ4058 profile we have three well defined peaks. The first one, at about −280 km s^{-1} if we assume a heliocentric radial velocity of WR 134 close to zero (see Sect. 1), is the blue component of the double peak discussed so far. Indeed it has perfectly matching equivalents on the He II lines λ4200 and λ4339. The next peaks of N IV λ4058, located at about −615 and −1170 km s^{-1}, again have matching features on the two He II lines (cf. Fig. 4 and Table 1).

Moving now to the red side of the variation spectrum of N IV λ4058 there are two well defined peaks at about +275 km s^{-1} and +865 km s^{-1}. On the He II λ4200 and λ4339 lines we have instead a much broader peak, the width of which includes the position of the two peaks observed for N IV λ4058, giving the impression of a blend resolved in the case of N IV λ4058 but not resolved in the case of He II λ4200 and λ4339.

The other lines present in the wavelength domain under investigation exhibit a much more complex and/or noisier structure. The He II λ4100 line is severely blended by N III $\lambda\lambda$4097, 4103 and Si IV $\lambda\lambda$4088, 4116, and maybe some other weaker lines. The next He II line of the series, He II λ4026 is blended with N IV λ4058 whose pattern of variability most probably extends as far as λ4030 if we assume an extension comparable to the one observed for He II λ4200 and λ4339.

The last line of the series, He II λ3968 has another problem. We suspect that the strong single peak in the variation spectrum refers to the Ca II λ3968 line. Of course the interstellar line does not vary, but this strong and narrow absorption line, with its sharp edges, introduces spurious variations linked to an insufficient spectral resolution. In other words, at the level of a wavelength bin, we have a small wandering of the position of the Ca II line, observed if we make a wavelength measurement of this line through a Gaussian fit on the individual spectra. This introduces a contamination on the variation spectrum of He II λ3968 which otherwise is broader and weaker.

A statistical study of the features in the variation spectrum may perhaps give some support to our conclusions. An F test of the ratio of variances can be used and we will assume the numbers of degrees of freedom as being both equal to 33. In this case, the 99.5% confidence level corresponds to the critical value $F = 2.54$ and the 97.5% level corresponds to $F = 2.01$. If we take the variance in the continuum (0.0034^2) as the reference, we conclude that everything above a standard deviation of 0.006 can be considered as significant deviations. If we consider the He II λ4200 line, the red peak in the variation spectrum corresponds to a variance of 0.016^2 whereas the central minimum is at 0.010^2: the ratio (2.62) indicates again a significant feature. This is a fortiori true for the central minimum of N VI λ4058. Finally, let us test the secondary peak at $-1170\,\mathrm{km\,s^{-1}}$ of that last line. It corresponds to a variance of 0.026^2 and, from neighbouring wavelengths, the expected value can be conservatively estimated to be 0.018^2. The ratio corresponds to a 97.5% confidence level implying that the associated feature is marginally significant and needs further confirmation.

The statistical analysis described above is not to be considered as rigorous, but rather as indicative because several basic hypotheses of the F test are clearly not fulfilled. First, some spectra (usually taken on the same night) are so similar that they can hardly be considered as independent. In addition, the basic signal has no reason to be Gaussian.

It is important to notice that this multi-peak structure is also present on the variation spectrum of N IV λ4058 derived from the Kitt Peak data, although less obviously due to the higher noise level. In addition to this confirmation from an independent data set, it will be shown later that the presence of local maxima and minima in the variation spectrum is directly related to the existence of the nodes which will be described later (Fig. 10).

In summary, the "variation spectrum" gives us the first constraints we have to take into account: the variability occurs preferentially at some specific Doppler shifts in several lines.

Another thing which is striking during an eye inspection of the collection of spectra is the similarity of the deformations on the various lines. This is particularly obvious for He II λ4200 and λ4339 as can be seen on Fig. 1, but it is also true for other lines. Again this feeling can be systematized. The procedure consists, on every individual mean-normalized spectrum, to take the pattern of a relatively unblended line (i.e. He II λ4200) and to move it along the spectrum while trying to cross correlate it with the encountered structures. This has been done for all the spectra of Fig. 3 and the result is amazing: it is given in Fig. 5 where we see something which looks like a nicely deblended spectrum of WR 134.

The wavelength positions of the "lines" of Fig. 5 have been measured relatively to the position of He II λ4200 (indeed in such a process we perform differential measurements and we get relative positions) and are given in Table 2. As can be seen we recover the laboratory wavelengths with an accuracy of the order of a tenth of an Ångström i.e. a fraction of a pixel. The largest difference

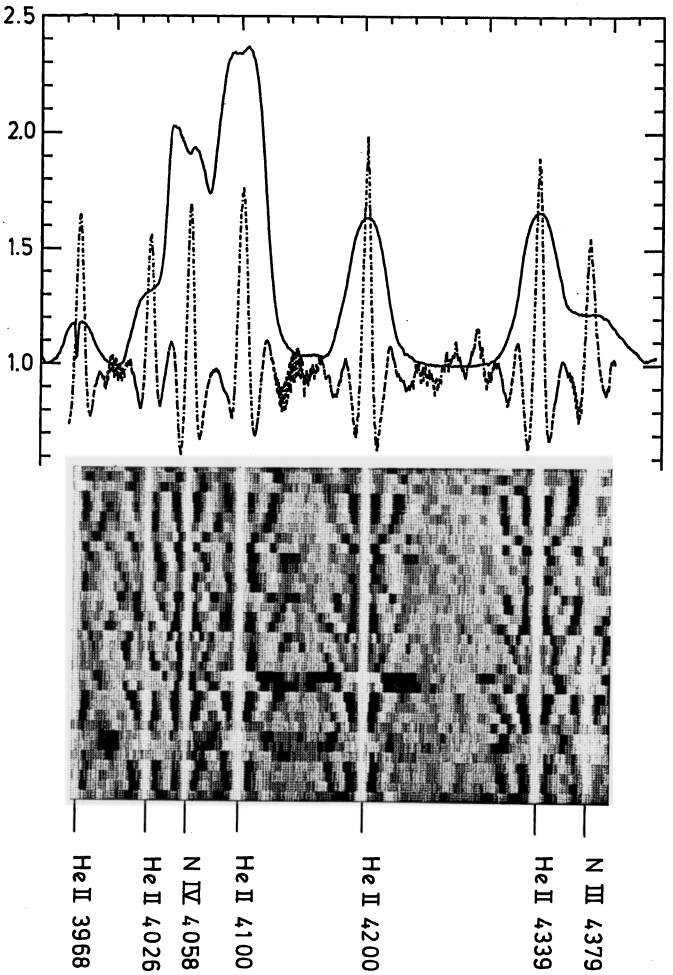

Fig. 5. Bottom: Result of local pattern cross-correlations on HPO mean-normalized spectra using the deformation pattern of He II λ4200 as reference. Grey corresponds to an absence of correlation. The various degrees of white (black) indicate the degree of the (anti-)correlation when the reference pattern is positioned at the wavelength under consideration (see text). Top: the dashed line is the mean of the results illustrated below shifted up by one unit, superimposed on the mean spectrum of Fig. 1

Table 2. Measurements of the relative positions of the patterns of line profile deformations observed on the mean-normalized spectra through cross-correlation with the deformation pattern of He II λ4200

Laboratory wavelengths (Å)	Pattern cross-correlation wavelengths (relative to He II λ4199.83) (Å)	Difference (Å)
He II 3968.43	3968.78	+0.35
He II 4025.60	4025.64	+0.04
N IV 4057.80	4057.89	+0.09
He II 4100.04	4100.13	+0.09
He II 4199.83	4199.83 [a]	0.0 [a]
He II 4338.67	4338.54	−0.13
N III 4379.11	4379.30	+0.19

[a] By definition.

(~0.35 Å) is obtained for He II λ3968 but remains less than a pixel (for HPO data 1 pxl is roughly equivalent to 1 Å). This indicates that the problem generated by the interstellar Ca II λ3968 line on the variation spectrum is no longer critical here as it concerns a bandwidth which is much smaller than the width of the pattern used for the cross correlation. It is interesting to notice that these differential measurements of the localization of the variability pattern lead to a result completely different from the one obtained with the measurements of the line "centers" as performed by McCandliss (1988) or Underhill et al. (1990) who get different Doppler shifts for different lines.

The study of variability happens to be an expensive but powerful way to deblend some lines in Wolf-Rayet spectra, the variable ones, at least for identification purposes. Before leaving Fig. 5 it is interesting to notice that we get a single and precise position for N IV while the mean spectrum clearly shows a double peaked structure (see later).

Figure 5 shows another result we have to take into account: although it is not exactly the same volume of wind which contributes to the formation of the different lines (see for example Hillier 1987), the deformations of the profiles are produced in a set of localized zones which is nearly the same for all the lines of Fig. 5. Otherwise we would get strong Doppler and/or time delays and the nice results of Fig. 5 and Table 2 would not emerge. Nevertheless, if this applies to the line of Fig. 5, it does not to the He I lines. As pointed out by McCandliss (1988), for these lines the variation detected on the emission part of their profiles is marginally higher than the one observed in the continuum i.e. barely detectable. This fact has been confirmed by Underhill et al. (1990) in the case of He I λ5876. Nevertheless a clear signature is found in the absorption component of P Cygni profiles of He I λ5876 and He I λ4471 (McCandliss 1988).

There are other results to be taken into account. First, the variability exists also far away in the wind as shown by the analysis of the absorption components of P Cygni profiles. Second, the variability at low Doppler shift chiefly observed in the N IV λ4058 and He II lines gives no apparent signature on the He I line profiles. This indicates that the related phenomenon takes place in such conditions that there is no – or at least very little – production of He I emission lines and/or that the spatial extent of this phenomenon is negligible compared to the emitting volume of the He I lines. The reverse is not true in the sense that at the large Doppler shifts of the detected He I variability ($\sim -1600\,\mathrm{km\,s^{-1}}$) we continue to see variability on the He II and N IV λ4058 lines but with a relative intensity weaker than the one seen close to the line center. This indicates that the ratio between the coherently varying part of the emitting volume and the rest of the same volume decreases when the Doppler shift increases i.e. while moving away from the star. Looking at a given Doppler shift on an absorption component is a way to reduce the volume under consideration i.e. to increase the probability of coherence.

Leaving variability and turning our attention to the mean spectrum, its inspection turns out to be instructive. As shown in Fig. 1 and even better in Fig. 6 where He II λ4026 line has been removed, one sees that N IV λ4058 is double peaked. The handling of the blending of the red wing of its profile is less secure for two reasons. The first one is linked to the existence of many components in the blend, namely He II λ4100, N III λλ4097, 4103 and Si IV λλ4088, 4116. The second reason is the uncertainty concerning the intensity of the He II λ4100 line without elaborate modelling as we precisely are dealing with the limit between optically thin and optically thick lines in the coarse analysis vocabulary of Castor & Van Blerkom (1970). What is important is

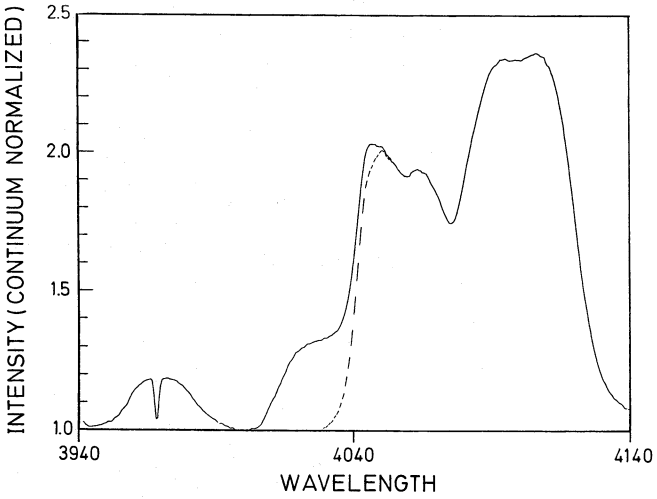

Fig. 6. Result of a partial deblending of N IV λ4058

that any attempt to remove the He II λ4100 line from the blend keeps a double peaked profile for N IV λ4058. Nevertheless its width at half intensity (using the blue slope of the profile and assuming a zero Doppler shift of the line center) is quite comparable to the one of the He II lines. What is interesting to notice is that the positions of the two peaks of the mean profile do not coincide with the positions of the two main peaks of the variation spectrum. This is another result we have to take into account.

In connection with the problem of the evaluation of the intensity of He II λ4100, another important characteristic of WR 134 needs to be mentioned. When our own measurements (or the ones of Castor & Van Blerkom 1970) of the intensity of He II lines of the 4-*n* series are plotted as a function of *n*, they lead to a graph similar to the one of Fig. 11 c of Conti et al. (1983), i.e. these measurements confirm that the intensities of the He II lines of the 4-*n* series issued from an upper level with an even *n* define a locus which lies below the one obtained from the lines of the same series but corresponding to odd values of *n*. Such a coherence between three independent determinations tends to indicate that, although very weak, this effect is real and is not the result of inescapable slight errors in the measurements, as assumed by Conti et al. (1983). This effect could be due to line blending, but until now such an argument has been used to explain the opposite situation i.e. a reinforcement of the lines issued from upper levels corresponding to even values of *n* (Bhatia & Underhill 1986). If such "à la carte" unknown blendings are not the answer, we are left with the possibility that, as for the situation where there is a relative reinforcement, the perturbing agent is H. But in the present case the H lines should be in absorption, not in emission. The interesting implication would be that some parts of the wind which are located between the star surface and the observer are sufficiently transparent to allow some access to the photosphere (see Sect. 4 for a possibility). But the mechanism responsible for the observed variability is not localized at the H photospheric level since no difference is observed between the variability of He II lines corresponding to odd or even values of *n*. It is the He II emission which is varying, not the H absorption.

Coming back to the variability it is interesting to leave for a while its statistical analysis and have a look at a few individual spectra. To examine a series of spectra taken during a given night is indeed the only way to obtain information on the evolution of a given perturbation.

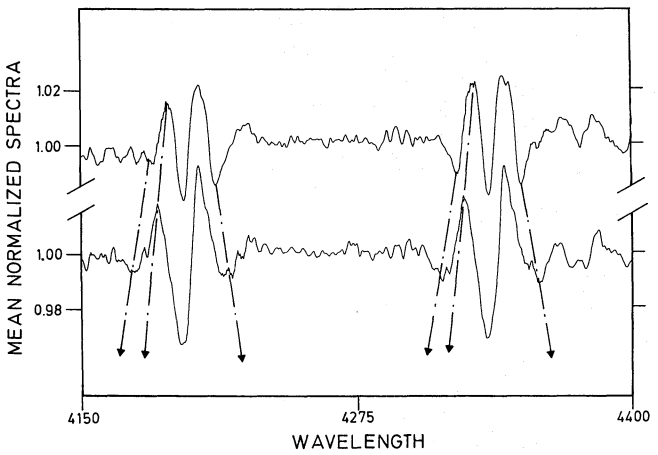

Fig. 7. Example of deformations (July 31, 1987) slightly drifting away from line center as time increases. The arrow indicates the direction of motion. The time interval between the mean-normalized spectra shown is 3 h 20 min

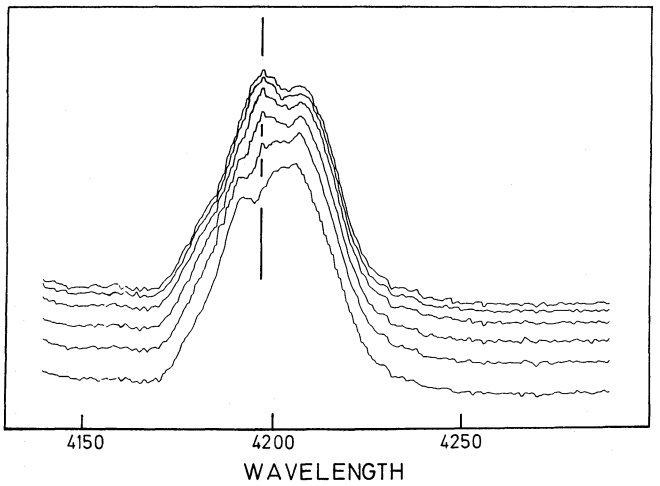

Fig. 8. Example of a deformation growing in situ (August 5, 1987) as can be seen on direct spectra. The shift of the continuum level is proportional to the time interval. Time is running from bottom to top. The vertical line draws attention to the Doppler shift stability of the small peak which appeared on the second spectrum (time interval between the second spectrum and the last one is 4 h 16 min)

As a matter of fact some events are rather close to Moffat et al.'s (1988) description in the sense that we see a kind of perturbation moving away from the line center while it develops to the blue as well as to the red (Fig. 7). On this figure are plotted two mean-normalized spectra of July 31, with arrows indicating the motion as time progresses, for the main perturbations on the He II lines. For clarity, only two spectra have been plotted, but the two others of the same night fit the variation. Such a motion is easier to see on mean-normalized spectra than on "true" spectra where the varying slope of the underlying profile complicates the situation. The displacements shown on this figure are the maximum we have observed. The arrows have been lengthened for the clarity of the figure: we have no observational evidence that the displacements can be extrapolated i.e. no observational evidence that the maximum Doppler shift excursion of a local maximum can be larger than the one illustrated by the two tracings shown in Fig. 7. Instead we have evidence that a complete "reversal" (i.e., at a given wavelength, the transformation of a local maximum into a local minimum) can occur on a short timescale (see below, Fig. 10).

As pointed out by Underhill et al. (1990) some events differ markedly from the one illustrated in Fig. 7 and are better described as the appearance of a perturbation which then remains stable in wavelength during many hours as shown in Fig. 8 where the spectra of August 5 have been plotted. Here the problem mentioned above (i.e. the varying slope of the underlying profile in case of Doppler drifting of the perturbation) is no longer present, and it is possible to show such an event on direct spectra. In addition, it is also interesting to notice in this figure that, while the central part of the narrow peak defining the perturbation remains stable in wavelength, the blue wing of the peak is progressively expanding to the blue.

The next two figures we wish to show are not unique in our data. On the first one (Fig. 9) are two examples of how precisely a given variability pattern on a mean-normalized spectrum can repeat itself after some time. The second figure (Fig. 10) shows two examples of two variability patterns which are nearly the mirror image of one another: on each example the loci of intensity excesses of the first mean-normalized spectrum coincide nearly perfectly, even in a kind of reverse shape, with the loci of intensity

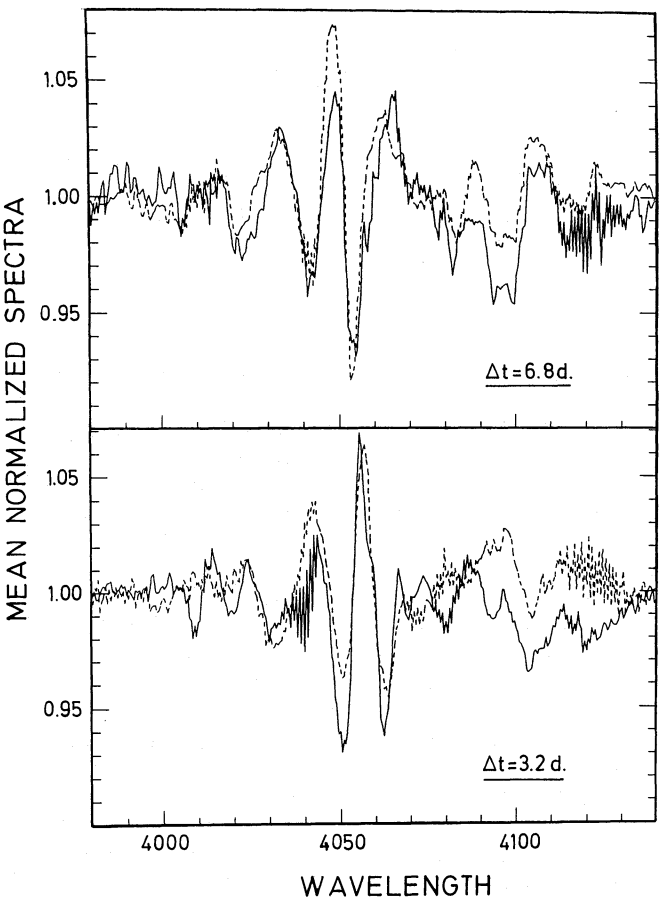

Fig. 9. Examples of the quality of the repeatability of a given deformation pattern, even after several days

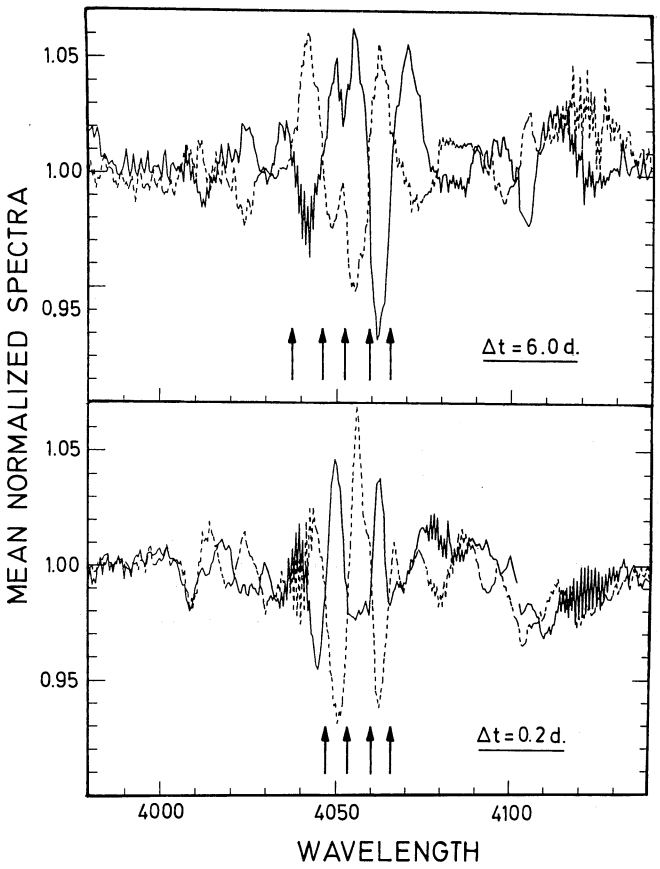

Fig. 10. Examples of two deformation patterns which give the impression of a "mirror" situation. The lower arrows indicate the positions of the nodes: they correspond to the local minima on the variation spectrum of Fig. 4

depletions of the second one (observed in one case a few hours later).

These two figures also give the impression of nodes in the process, a concept already encountered in the discussion of the variation spectrum. The positions of the nodes of Figs. 9 and 10 are not "iron fixed": there are events during which the nodes occupy a different position although statistically they tend to preferentially occur at some given Doppler shifts. A quick "reversal" during the night, as illustrated in the bottom part of Fig. 10, gives a clear definition of the nodes. Instead, a situation of "moving blobs", as illustrated in Fig. 7, i.e. a situation during which the perturbations drift away while developing, is an event which introduces some blurring in the definition of the nodes and explains why the minima of the variation spectrum are not deeper. These figures also illustrate another rather systematic trend i.e. the fact that most of the time there is a node located close to the rest wavelength, and that there is a frequent anticorrelation between the blue and red deformations. There is a slight wavelength shift in the position of this central node as observed in HPO or KPNO variation spectra. It is possible that this shift has no deep meaning and results from a slight difference in the distributions of variances around the two main maxima ("red" and "blue"). Nevertheless it would be interesting to accumulate more data in order to investigate this problem and to check the stability of the position of the local maxima and minima on the variation spectrum.

4. Towards a possible interpretation

If we consider the indications derived in the previous Sect. (3) one of the most constraining is the existence of preferential Doppler shifts for the appearance of the profile deformations. This leads us to rule out many of the usual models. There is no reason to have preferential Doppler shift zones in the case of accelerating "puffs". We can imagine a limited Doppler shift domain for their visibility due to contrast problems but we can hardly imagine the appearance of a node-like pattern. Again this constraint is difficult to handle if the observed deformations are linked to disturbances like spots or eddies either corotating with the star or moving randomly at its surface or at some distance in the wind. The same applies for a disturbance located on a rotating disk where again an uninterrupted sweeping of the whole Doppler shift domain is expected.

Instead we need to consider a scenario in which a particular mechanism takes place in specific regions of the wind characterized by given Doppler shifts relative to the observer. A way to do it is through the existence of some kind of jets if their position is stable relative to the observer and if the mechanism responsible for the observed variability can take place only at some given locations in the jets, at some given distance from the star's surface. This way we get a spatial node pattern which "projects" itself into a node pattern on a Doppler shift scale if we keep the usual scenario of an accelerating wind.

If we imagine a bipolar jet, its axis must be inclined relative to the observer as we need to see the receding jet, i.e. the one containing the material flowing away from the observer. But the inclination must be rather small if we assume that the variability observed in the absorption component of the P Cygni profile is of the same nature (i.e. linked to the jets) as the one observed at smaller Doppler shifts on the emission line profiles (something which is not proven). In such a hypothesis the inclination of the axis relative to the line of sight must be smaller than the opening angle of the jet. This is the situation we have tried to sketch in Fig. 11.

If the variability observed at large distances (in the absorption components of P Cygni profiles) is of another nature (i.e. is not linked to the jets), then it is no longer necessary to keep a very small inclination of the polar axis relative to the direction to the observer. This allows one to have a much faster acceleration of the wind as there is no longer a severe occultation problem at the base of the receding jet (the first shock observed in the receding jet has a rather small velocity shift but its minimum acceptable distance from the star is a function of the jet's inclination relative to the observer's direction). Also of importance to derive constraints for the inclination of the jets and the acceleration law in that region would be more quantitative information from the polarimetric observations notably about the degree of oblateness.

A way to keep material flowing in jets is through the existence of magnetic fields: we will then assume that there is a bipolar magnetic field whose axis coincides with the axis of the bipolar jet. As a matter of fact, while trying to understand the variability of the line profiles of WR 134, we come very close to a model recently suggested by Poe et al. (1989) in another context. This is a rotating, magnetic, radiation-driven wind model which is no longer spherically symmetric: there is a slower but denser equatorial flow and a fast radiation-driven wind at higher latitudes. In connection with our remark concerning the intensity of the lines of the He II 4-*n* series let us also mention that in this paper the possibility of seeing the hydrostatic surfaces of the Wolf-Rayet stars and consequently intrinsic photospheric absorption lines is also raised. But the most

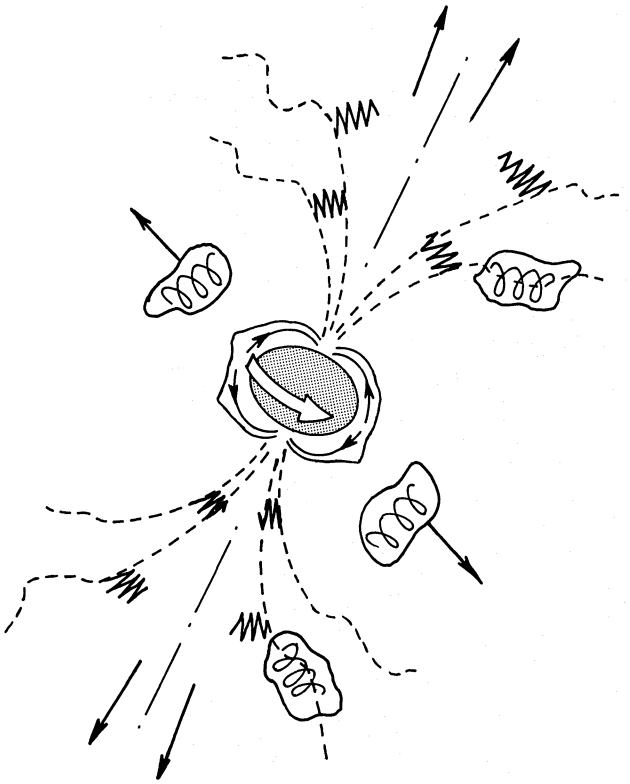

Fig. 11. Schematic view of the proposed model. The observer is seeing the figure from the bottom. The flattening of the central disk is due to rotation. In the regions around the magnetic axis, the plasma moves more or less freely away from the star. Nevertheless, at times, shocks develop, preferentially at some given distances from the star i.e. at preferential Doppler shifts (they are represented by sharp zig-zags in the figure). At the shock location, the magnetic field configuration is temporarily destroyed. Plasma clouds, with frozen-in magnetic field lines, are formed and then drift away under the influence of the gradient of radiation pressure. The opaque central disk represents, for the high density wind region, these inner layers where the magnetic field strongly controls the plasma motions. Outside that region, the two solid lines, more or less concentric, are located in the assumed region of formation of a sizeable part of the N IV λ4058 emission. The arrows on the inner solid line indicate the net current flowing away from the equatorial region towards the pole (see text). This region is assumed to include the border of the magnetically controlled part of the atmosphere. On that border, pockets of plasma, with frozen-in magnetic field lines are constantly formed and then drift away, generating inhomogeneities in the wind structure outside the polar regions (the shocks are related to the inhomogeneities in the polar region)

interesting aspect of this model for the present discussion is the existence of the fast low density flows in the two polar regions. There is no reason to expect to have such a flow accelerating smoothly until the terminal velocity (see for example the work of Owocki et al. 1988, even if it concerns another geometry and different constraints: spherically symmetric isothermal radiatively driven flow). Intuitively we can consider that the open field lines close to the polar axis act as an imperfect nozzle. In a badly shape mechanical nozzle a shock develops at a given distance in the flow. Here, the situation is different. First, there is the permanent source of acceleration provided by the gradient of radiation pressure. Another important difference arises from the fact that the "walls" of the nozzle are not rigid and most probably the plasma induces perturbations in the magnetic field line configuration at the location of the shock. This could explain why we have more than one shock region in the jet and also why the shock, sometimes, develops itself at a relatively stable distance from the star, or, sometimes, drifts away while developing, depending on the complex balance between the energy of the plasma and that of the magnetic field. The deformation of the magnetic field line configuration during the shock should also play a role in the dissipation process of the shock and, consequently, in the post shock physical conditions which could find a signature in the observed intensity decreases mirroring the intensity increases.

The existence of these shocks could be intrinsic to the very process of the flow itself: an accelerating supersonic flow in an imperfect nozzle and/or trajectory readjustments of the external layer of the jet. In the jet the kinetic energy of the accelerating plasma is constantly increasing with the inescapable consequence that after some distance that kinetic energy overrides the magnetic energy available for the control of the trajectories by the magnetic field configuration. Such a competition takes place in the external parts of the jet, not in its inner core. One can imagine that this could happen regularly, smoothly, or discontinuously in which case the signature of the readjustments would be the observed variability. Nevertheless in such a context it is difficult to deal with the observed rather systematic anticorrelation between the deformations located on both sides of the rest wavelength.

But the shocks could also be triggered more or less regularly by variations of the total amount of matter injected at the base of the nozzle. These variations themselves could be induced by a deep mechanism acting at the very base of the flow, i.e. at the level of the surface of the star. They could also be the result of matter injection in the nozzle at some distance from the surface, injection linked to the sporadic opening of closed magnetic field lines (of magnetic bottles) located in the transition layer which separates the region totally controlled by the energy of the magnetic field from the one where the kinetic energy of the plasma dominates. In this hypothesis some of the variable amount of matter injected in the nozzle could originate from the equatorial region.

In such a context we could very tentatively try to deal with the peculiar aspect of the N IV λ4058 line i.e. its double peaked structure on the mean spectrum. This could be linked to the fact that a sizeable fraction of the emission region of this line coincides with the transition layer mentioned above, transition from the closed field (with no radial flow) to the open field (with expansion and mass loss). This means that a sizeable part of the N IV λ4058 emission would be produced in a fast rotating hollow shell, a situation which is reminiscent of the ring suggested by Underhill et al. (1990) except that here the shell is very close to the star's surface. The double peaked aspect could also result from the motions of ions bouncing back and forth in a configuration of closed field lines. If so, the central part of the profile would be depleted because, for a given ion, a zero Doppler shift relative to the observer occurs near the two magnetic mirrors of the ion's trajectory (in any case, away from the equator); but we can see only one, the other one being occulted by the star. Of course any mechanism leading to the double peaked aspect of the N IV λ4058 profile is also operating for any other ion existing in the same spatial region and the different aspect of the line profiles can only result from the differences in the relative extensions of the emission volumes. Nevertheless so far there is no explanation for the strong asymmetry observed on the N IV λ4058 profile i.e. for the fact that the blue peak is markedly stronger than the red one. A way to obtain the latter effect is to assume that there is a net current of particles flowing from the equator region toward the poles, with only a part of them bouncing back. In such a picture the lower intensity of the red peak would simply result from an occultation effect.

Finally, the reason for the quasi lack of observed variability in the emission component of the He I lines is probably due to the fact that there is no way to produce a He I line under the physical conditions prevailing in the first shocks. The physical conditions to get a He I line emission are only encountered much farther away from the star (at a distance of more than five stellar radii while an He II line like He II λ4200 has its maximum contribution well below this limit, if we refer to a model by Hillier 1987).

We do not claim that we have proven that this scenario is the clue to the variability of WR 134 but at least we have suggested a solution which more or less fits all the constraints listed in Sect. 3, which, in fact, are not so easy to deal with.

As a last point let us also recall the observations of the He I λ10830 profile by Vreux et al. (1990) and by Eenens (1990). Both show an extra emission located at the redward limit ($+1100\,\mathrm{km\,s^{-1}}$) of the rather flat-topped emission component of a P Cygni profile. This emission is a narrow one according to Eenens (1990) who has higher resolution data than Vreux et al. (1990). Again these narrow emissions superimposed on top of the He I λ10830 profiles in some Wolf-Rayet stars have been suggested to be the signature of jets (Eenens 1991). On the WR 134 spectra, the lack of an obvious signature of the jet flowing towards the observer can either be due to the absorption component of the P Cygni which would be partially filled in by that extra component of the emission, or it is due to an asymmetry in the amount of material carried by the two components of the bipolar jet.

Acknowledgements. We appreciate the allocation of observing time at Haute Provence and Kitt Peak Observatories. Discussions with P. Eenens, R. Scuflaire and W. Schmutz are gratefully acknowledged, as well as a reading of the manuscript by J.P. Swings and detailed refereeing by A. Moffat. This research has benefited from NATO Collaborative Research Grant 0116/88 to J.-M.V., B. B. and P. C. It has also been partly supported through a grant of the Fonds National de la Recherche Scientifique to J.-M.V. and through contract ARC 90/94–140 "Action de Recherche Concertée de la Communauté Française" (Belgium). J.-M.V. has also appreciated the hospitality of J.I.L.A. during his stay in Boulder.

References

Antokhin I.I., Aslanov A.A., Cherepashchuk A.M., 1982, Sov. Astron. Lett. 8, 156
Antokhin I.I., Volkov I.M., 1987, Inf. Bull. Var. Stars, no. 2973, 1
Balona L.A., 1986, MNRAS 219, 111
Bhatia A.K., Underhill A.B., 1986, ApJS 60, 323
Castor J.I., Van Blerkom D., 1970, ApJ 161, 485
Chu Y.-H., Treffers R.R., Kwitter K.B., 1983, ApJS 53, 937
Conti P.S., Leep E.M., Perry D.N., 1983, ApJ 268, 228
Eenens P.R.J., 1990, private communication
Eenens P.R.J., 1991, In: The infrared spectral region of stars, Jaschek C., Andrillat Y. (eds.) Cambridge University Press, p. 137
Hillier D.J., 1987, ApJS 63, 965
Lamers H.J., Snow T.P., de Jager C., Langerwerf A., 1988, ApJ 325, 347
Lamontagne R., 1983, Ph.D. Thesis, Université de Montréal
McCandliss S.R., 1988, Ph.D. Thesis, University of Colorado
Moffat A.F., Shara M.M., 1986, AJ 92, 952
Moffat A.F., Drissen L., Lamontagne R., Robert C., 1988, AJ 334, 1038
Owocki S.P., Castor J.I., Rybicki G.B., 1988, ApJ 335, 914
Poe C.H., Friend D.B., Cassinelli J.P., 1989, ApJ 337, 888
Ramsey L.W., Huenemoerder D.P., 1986, Proc. SPIE 627, 282
Robert C., Moffat A., Bastien P., Drissen L., St. Louis N., 1989, ApJ 347, 1034
Scargle J.D., 1982, ApJ 263, 835
Schmidt G.D., 1988, In: Polarized radiation of circumstellar origin, Coyne G.V. et al. (eds.) (Vatican), p. 641
Smith L.F., Kuhi L.V., 1970, ApJ 162, 535
Treffers R.R., Chu Y.-H., 1982, ApJ 254, 569
Underhill A.B., Gilroy K.K., Hill G.M., Dinshaw N., 1990, ApJ 351, 666
van den Heuvel E.P., 1976, Late stages of close binary systems. In: Structure and Evolution of Close Binary Systems, IAU Symp. 73, Eggleton P. et al. (eds.), Reidel, Dordrecht, pp. 35–61
van der Hucht K.A., Conti P.S., Lundström I., Stenholm B., 1981, Space Sci. Rev. 28, 227
Vreux J.-M., Andrillat Y., Gosset E., 1985, A&A 149, 337
Vreux J.-M., Manfroid J., 1985, Inf. Bull. Var. Stars, no. 2821, 1
Vreux J.-M., 1985, PASP 97, 274
Vreux J.-M., Andrillat Y., Biémont E., 1990, A&A 238, 207